

HORIZON 2020

Research Infrastructures

H2020-INFRAIA-2014-2015

INFRAIA-1-2014-2015 Integrating and opening existing national and regional research infrastructures of European interest



ENSAR2

European Nuclear Science and Application Research 2

Grant Agreement Number: 654002

## **D14.1: Report on performances of the EBIS debuncher**

*PROJECT AND DELIVERABLE INFORMATION SHEET*

ENSAR2 Project Ref. N <sup>o</sup>	654002
Project Title	European Nuclear Science and Application Research 2
Project Web Site	<a href="http://www.ensarfp7.eu/">http://www.ensarfp7.eu/</a>
Deliverable ID	D14.1
Deliverable Nature	Report
Deliverable Level*	PU
Contractual Date of Delivery	February 28 <sup>th</sup> 2018
Actual Date of Delivery	February 27 <sup>th</sup> 2018
EC Project Officer	Mina Koleva

\* The dissemination level are indicated as follows: PU – Public, PP – Restricted to other participants (including the Commission Services), RE – Restricted to a group specified by the consortium (including the Commission Services). CO – Confidential, only for members of the consortium (including the Commission Services).

*DOCUMENT CONTROL SHEET*

Document	Title: Report on EBIS debuncher performances	
	ID: D14.1	
	Version 1	
	Available at: <a href="http://www.ensarfp7.eu/">http://www.ensarfp7.eu/</a>	
	Software Tool: Microsoft Office Word 2007	
	File: ENSAR2_Deliverable_EBIS-debuncher_20180227	
Authorship	Written by:	Predrag Ujic
	Contributors:	Pierre Delahaye
	Reviewed by:	Fredrik Wenander, Krzysztof Rusek
	Approved by:	

*DOCUMENT STATUS SHEET*

Version	Date	Status	Comments
1	30.01.2018	For internal review	
2	08.02.2018	Reviewed	
3	14.02.2018	2 <sup>nd</sup> reviewer	
4	27.02.2018	Submitted on EC Participant Portal	
		Final version	

*DOCUMENT KEYWORDS*

Keywords	debuncher, charge breeding, electron beam ion source, continuous wave beams
----------	---

**Disclaimer**

This deliverable has been prepared by the Innovative Charge Breeding Techniques (ICBT) task within Work Package 14, EURISOL JRA of the Project in accordance with the Consortium Agreement and the Grant Agreement n°654002. It solely reflects the opinion of the parties to such agreements on a collective basis in the context of the Project and to the extent foreseen in such agreements.

**Copyright notices**

© 2016 ENSAR2 Consortium Partners. All rights reserved. This document is a project document of the ENSAR2 project. All contents are reserved by default and may not be disclosed to third parties without the written consent of the ENSAR2 partners, except as mandated by the European Commission contract 654002 for reviewing and dissemination purposes.

All trademarks and other rights on third party products mentioned in this document are acknowledged as own by the respective holders.

## TABLE OF CONTENTS

*DOCUMENT KEYWORDS* .....2

Disclaimer .....3

Copyright notices .....3

List of Figures .....4

References and applicable documents .....5

List of acronyms and abbreviations .....6

Executive Summary .....7

Introduction .....7

The Beam Debuncher Prototype .....7

Test Description .....9

    Debunching test with successive linear ejection ramps (December, 2017 test) .....11

        Efficiency tests .....11

        Debunching test .....12

    Debunching test with inverse distribution function method (January 2018 test) .....13

        The method .....13

        The efficiency test .....14

        The 10 ms debunching signals .....16

        The 100 ms debunching signals .....17

        The 0.8 s debunching test .....19

Conclusions .....20

## LIST OF FIGURES

Figure 1. Drawings of the debuncher prototype and its main parts. Entrance and exit gate electrodes have X-shaped fingertips in order to increase the transmission efficiency. ....8

Figure 2: Debunching sequence. The dashed lines represents the voltages applied to the successive group of segments (see Figure 3) of the trap and the injection electrode (in arbitrary units). The Micro-Channel Plate (MCP) signal of detected Cs ions, as observed on the oscilloscope, is shown as the solid blue line. The signal polarization is negative, with a base level of about 14 mV. ....9

Figure 3: The grouping of the 23 internal electrodes of the debuncher used in the tests (December 2017 and January 2018 test – see the text for details). There are 8 groups of DC segment, each with a time-varying HVx potential. ....10

Figure 4: Number of extracted ions as function of the trapping time (the intensity of injecting beam was constant). .....	11
Figure 5: HV platform oscillations induced by the arbitrary waveform generator superimposed with the the inherent ripple from the main high voltage power supply. On the x-axis one major unit corresponds to 400 ns and on the y-axes 1 V. ....	12
Figure 6: Li ions ejected by subsequent use of linear potential ramps analogue to the ones used in the EMILIE debunching test with a period time of 12.5 ms (see Figure 2).....	13
Figure 7: Method adapted from Lapiere [5]. $R_i$ is a constant rate of ion extraction (see [5] for details) and the $R_{it}$ corresponds to the lowering rate of the exit DC gate. Instead of lowering the potential of the exit gate, we increased the potential of the inner DC electrodes inside the trap to produce the debunched beam.....	14
Figure 8: Trapping efficiency test for ${}^7\text{Li}^{1+}$ ions with a lower ion energy (30 eV) showed that there is no significant losses at longer trapping duration, contrary to what was seen for ion energies of 70 eV (see Figure 3). ....	14
Figure 9: Time-of-flight as a function of the trapping time. The average ion velocity changes by a factor 2 between short trapping times (around 10 ms) and a 1 s trapping time. ....	15
Figure 10: Root mean square (RMS) of the time-of-flight as a function of the trapping time.....	16
Figure 11: (a) The axial momentum distribution of ${}^7\text{Li}^{1+}$ ( $E=30$ eV) measured by applying a linear ramp potential to the ejecting DC electrodes; obtained from step 2 in Figure 7. (b) The inverse integral distribution (step 5 in Figure 7) and (c) the extracted beam, which exhibits a quite uniform intensity in time. ....	17
Figure 12: The potential introduced to the ground of the HV platform (January 2018 test), synchronized with the injection period.....	18
Figure 13: First 100 ms debunching run: The axial momentum distribution scanned by linear ramp potential during the trapping period of 100 ms (left-hand). The beam extracted by the inverse integral function (right-hand).....	18
Figure 14: Second 100 ms debunching run: The axial momentum distribution scanned by linear ramp potential during the trapping period of 100 ms (left-hand). The beam extracted by the inverse integral function (right-hand).....	19
Figure 15: 800 ms debunching: The axial momentum distribution scanned by linear ramp potential during the trapping period of 800 ms (left-hand). The beam extracted by the inverse function (right-hand). ....	19

## REFERENCES AND APPLICABLE DOCUMENTS

- [1] <http://www.emilie-eurisol.eu/emilie-workshop/files/emil-traykov>
- [2] SIMION®, Scientific Instrument Services, Inc., Idaho National Laboratory, USA
- [3] Optimizing charge breeding techniques for ISOL facilities in Europe: Conclusions from the EMILIE project, P. Delahaye, A. Galatà, J. Angot, J. F. Cam, E. Traykov, G. Ban, L. Celona, J. Choinski, P. Gmaj, P. Jardin, H. Koivisto, V. Kolhinen, T. Lamy, L. Maunoury, G. Patti, T. Thuillier, O. Tarvainen, R. Vondrasek, and F. Wenander, Rev. Sci. Instrum., 87, 02B510 (2016)
- [4] FASTER (Fast Acquisition SysTem for nuclEar Research), <http://faster.in2p3.fr/>
- [5] Time-dependent potential functions to stretch the time distributions of ion pulses ejected from EBIST, A. Lapiere, Canadian Journal of Physics, 2017, 95(4): 361-369, <https://doi.org/10.1139/cjp-2016-0716>
- [6] <https://github.com/ujic/DebuncherGUI>

## LIST OF ACRONYMS AND ABBREVIATIONS

CW	Continuos Wave
EBIS	Electron Beam Ion Source
ECR	Electron Cyclotron Resonance
HV	High Voltage
ICBT	Innovative Charge Breeding Techniques
MCP	Micro-Channel Plate
RF	Radio-Frequency
RFQ	Radio-Frequency Quadrupole
ToF	Time of Flight

## EXECUTIVE SUMMARY

The EBIS beam debuncher has been thoroughly tested with stable 1+ beam on the LPC Caen test bench. Trapping lifetimes well beyond 1s could be measured, and continuous extracted beams with maximum intensity variations of  $\pm 20\%$  could be obtained for extraction times as long as 800 ms. Projections for the use of such device with an operational EBIS are therefore encouraging.

## INTRODUCTION

During the last decade the EBIS (Electron Beam Ion Source) technology has established itself as a key method for preparation of radioactive beams for further post-acceleration and Europe has been until very recently the world-leader in the field. The ion production in an EBIS is based on electron impact ionization in a high-density electron beam. Depending on different parameters, each collision has a certain probability to further ionize the confined ion and to increase consecutively the charge state of the ion. The breeding period that is necessary for completion of the EBIS cycle can be as long as several 100 milliseconds and the typical pulse length of the extracted ions varies from 1  $\mu\text{s}$  to  $\sim 100 \mu\text{s}$ . Although the EBIS can function both in CW (Continuous Wave) and in pulsed mode, the latter mode is preferred due to its higher efficiency. On the other side, for the nuclear physics experiments, CW beams are preferred whereas bunched beams of the same average intensity tends to have larger dead-times, more pile-ups and random coincidences in the detectors due to the higher instantaneous counting rate at the moment of the beam bunch arrival.

Within the ICBT task, one of the goals is to develop a debuncher device for CW ion beam formation to be used at future ISOL facilities that employ EBIS charge breeding. This report addresses the feasibility of realizing an optimized continuous beam formation from an EBIS type charge breeder.

## THE BEAM DEBUNCHER PROTOTYPE

The main for this debuncher is to efficiently capture the ions being ejected from the EBIS and in a controlled manner then slowly, during a predefined period, release them to the post-accelerator. The debuncher prototype design started within the EMILIE project [1]. In this type of debuncher the ions are confined in radial plane by a linear radio-frequency quadrupole (RFQ) structure, and axial trapping is achieved by two DC gate electrodes at the axial ends of the debuncher (Figure 1). In contrast to normally operating RFQ cooler/bunchers where the entrance DC gate is constantly allowing for ions to enter, the entrance DC gate of the EMILIE debuncher is pulsed. The potential of the gate is low during the injection period and thereafter raised to a higher potential during the trapping and ion release phase. The gate

electrodes are made as four X-shaped fingertips (see the Figure 1) instead of full electrode as SIMION [2] simulations showed that the transmission could be significantly increased in this manner.

In principle, the CW extraction of the ions can be achieved by two methods:

1. By slowly lowering the potential of the exit DC gate electrode.
2. By increasing the potential of the DC segments inside the debuncher (see Figure 1), while the exit DC gate electrode has a constant potential.

The second method, although slightly more demanding regarding the technical design, is preferable since it provides a debunched beam with smaller energy dispersion throughout the complete extraction phase.

The operation of the debuncher device requires good vacuum conditions since losses due to collisions and charge exchange must be avoided. The total path of the trapped ions inside the debuncher is very long – of order of kilometers. In our test setup, pressures of  $10^{-7}$  mbar could be obtained, which were shown to be sufficiently good to avoid losses for up to 1 s for ions injected with a low energy into the trap ( $\sim 30$  eV). This situation would be different if one would be injecting multiply charged ions. In this case, vacuum of the order of  $10^{-11}$  mbar or below, as in the EBIS itself, would be required, and the use of better materials, ionic pumps or cryopumps would have to be considered.

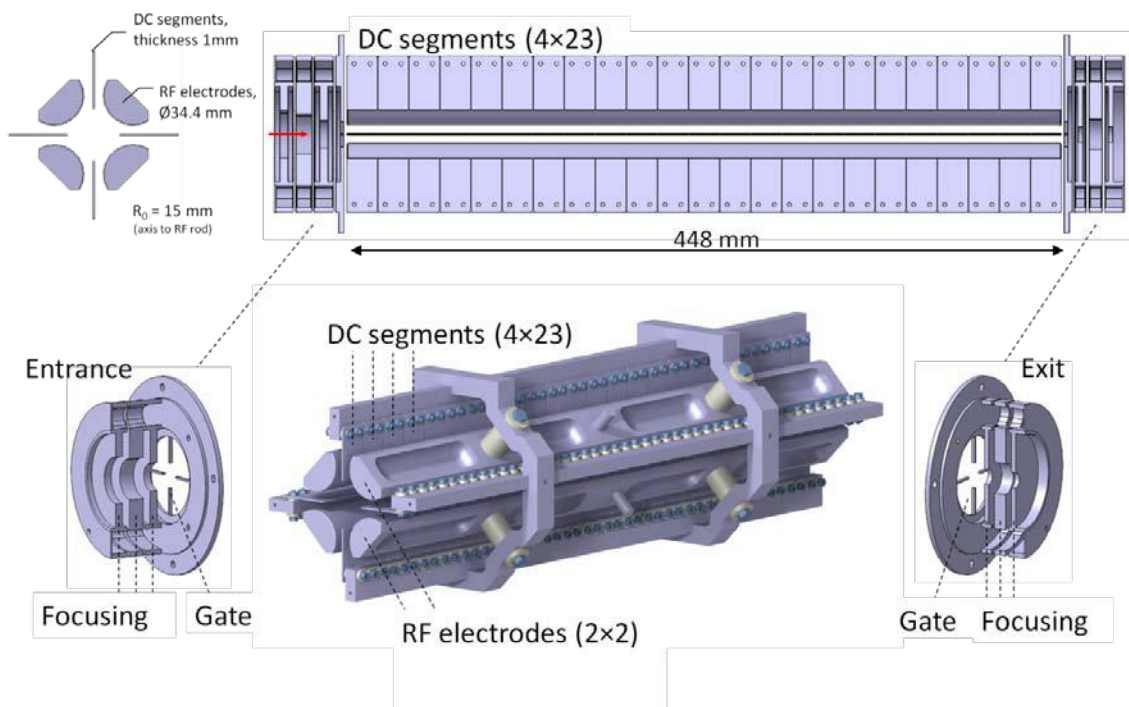


**Figure 1.** Drawings of the debuncher prototype and its main parts. Entrance and exit gate electrodes have X-shaped fingertips in order to increase the transmission efficiency.

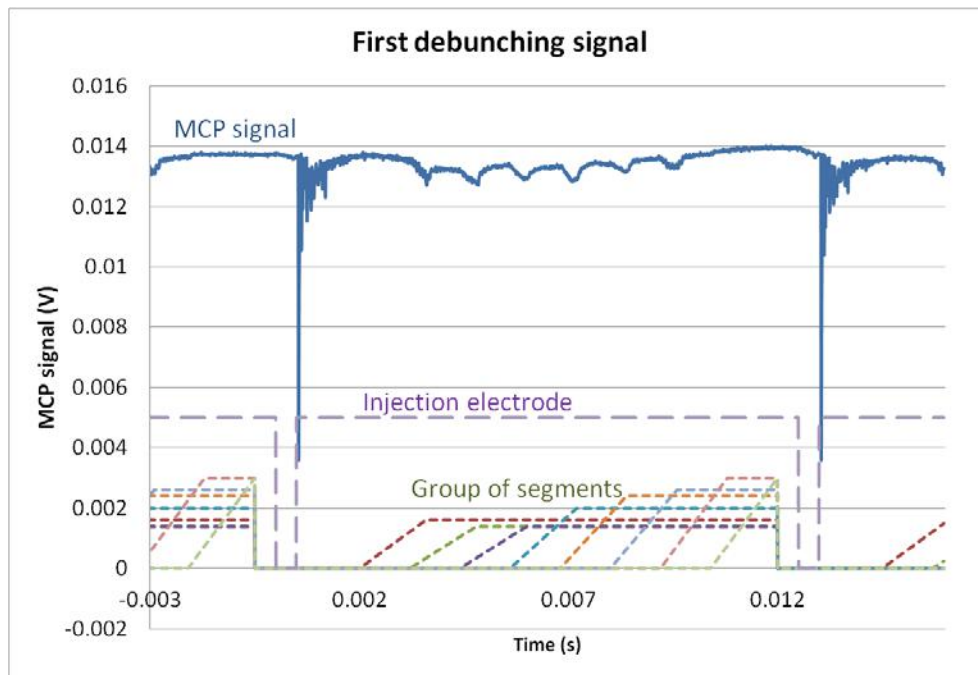


**Figure 2:** Debunching sequence. The dashed lines represents the voltages applied to the successive group of segments (see Figure 3) of the trap and the injection electrode (in arbitrary units). The Micro-Channel Plate (MCP) signal of detected Cs ions, as observed on the oscilloscope, is shown as the solid blue line. The signal polarization is negative, with a base level of about 14 mV.

The first debunching signals were obtained in the frame of the EMILIE project [3] (see Figure 2) with Cs ions. The ion extraction was conducted by successive potential increase of the DC segment groups inside the debuncher, from the injection side of the trap to the extraction side, as is schematically shown in Figure 2. Schematics of the grouping of DC segments is shown in the Figure 3 (to have in mind – the colors of DC segment groups in Figure 3 do not match the colors in Figure 2). The extraction time was limited to 12.5 ms cycles, and the resulting beam was not entirely continuous but rather a succession of slow pulses.

## TEST DESCRIPTION

In this report, we present an alternative extraction scheme and improved debunching results of an injected  ${}^7\text{Li}^{1+}$  beam for extraction periods of up to  $\sim 1$  s. The internal DC electrode segments of the debuncher were grouped and the extraction of a CW beam was made by applying different combination of time dependent DC potential. The groups of DC segments are shown in Figure 3.

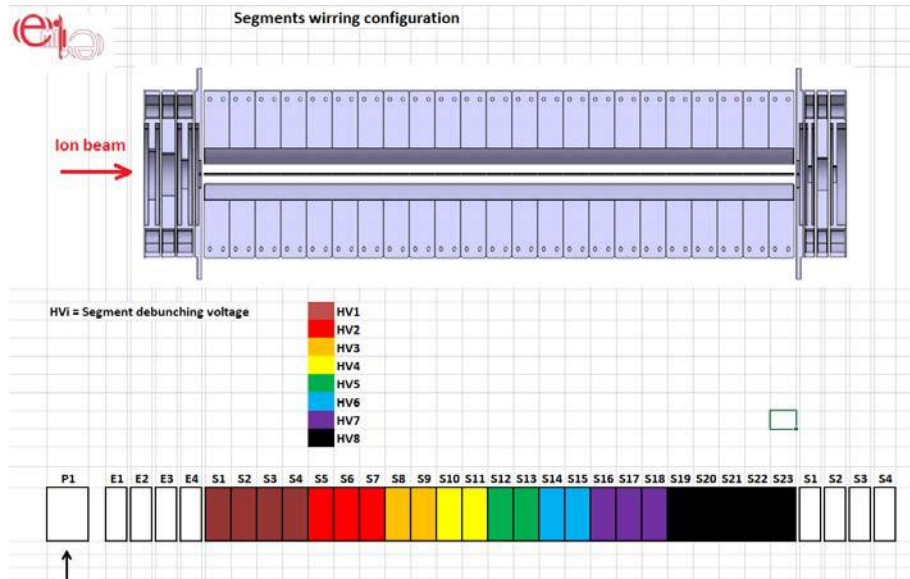


**Figure 3:** The grouping of the 23 internal electrodes of the debuncher used in the tests (December 2017 and January 2018 test – see the text for details). There are 8 groups of DC segment, each with a time-varying HVx potential.

The  ${}^7\text{Li}^{1+}$  ions have been chosen for the test due to their rather low  $A/q$ -ratio, close to the one that is usually required for reacceleration in post-accelerators. As an example, the CIME cyclotron at GANIL reaccelerates ions with  $A/q$ -ratio below 10. The  ${}^7\text{Li}^{1+}$  beam for the test is produced by a surface ion source with an energy of 5000 eV and beam intensities ranging between 0.1 and 200 nA. Beam bunches, as would be expected out of an EBIS, were emulated by switching on/off the entrance DC gate of the debuncher. The beam was injected into the debuncher during a period of 10 - 20  $\mu\text{s}$  and the extracted ions were detected by a MCP detector. The locally developed (LPC Caen) digital acquisition system FASTER was used for the acquisition of the extracted beam [4]. It is important to mention that the ion source and the HV platform of the debuncher were not biased at the same potential. The source, placed outside of the HV cage at the ground potential, had its own power supplies which were used to bias the hot surface emitting ions and an einzel lens for beam focusing.

In parallel to the experimental tests, simulations were carried out on the prototype design. The simulations were performed in the ion optics simulation program SIMION [2], which allows for customization by add-on programming. The latter was used for defining initial ion distributions and setting the time-varying parameters for the DC gates and the ejection potentials of the DC segments.

The debuncher test was conducted in two stages: December 2017 test and January 2018 test. The idea of the December 2017 test was to extend the debunching signals from 12.5 ms (as used during the test within the EMILIE project [3], Figure 2) to a few hundreds of ms, using the same linear ramp potential technique as for the EMILIE test [3]. As the result of the December 2017 test was not satisfying, in January 2018, a different extraction technique was utilized. The applied potentials of the DC segment groups during the extraction phase corresponded to the inverse function of the energy distribution of ions inside the trap. This method is similar to what was recently applied by Lapierre for the LEBIT facility [5] and will be detailed later.

## DEBUNCHING TEST WITH SUCCESSIVE LINEAR EJECTION RAMPS (DECEMBER, 2017 TEST)

### EFFICIENCY TESTS

Prior to the debunching test, trapping efficiency measurements were performed. Ions with an energy of 70 eV, relative to the debuncher potential, were injected into the trap. The potential of the exit DC gate was  $\sim 420$  V. Under these conditions, significant ion losses were recorded for trapping periods exceeding 10 ms (see Figure 4). Increasing the trapping potentials on the gate electrodes did not lower the losses, indicating that the ion loss process occurred in the radial plane. At this stage, the reason for the losses observed during this test remains to be investigated.

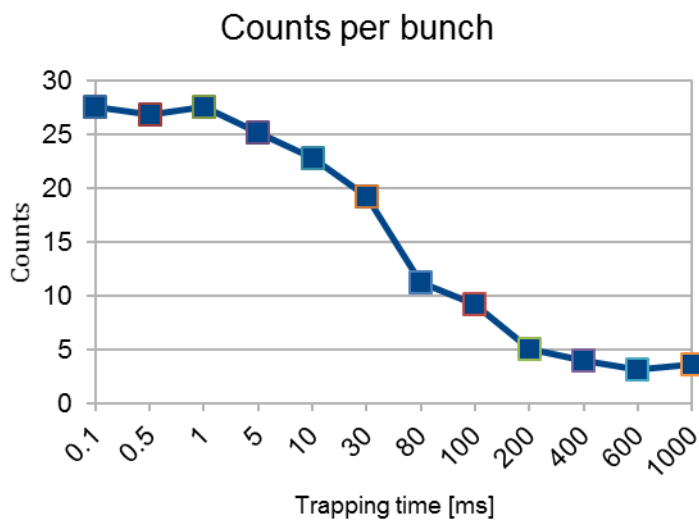


**Figure 4:** Number of extracted ions as function of the trapping time (the intensity of injecting beam was constant).

If the vacuum pressure is approximately  $10^{-7}$  mbar (assume air mixture), a 50 cm long volume contains  $\sim 10^{17}$  atoms/cm<sup>2</sup>. The velocity of the Li ion having an energy of 70 eV is of order of 4 cm/ $\mu$ s. During the trapping time of 100 ms the path length will be  $\sim 4$  km, which means the Li ion will pass back and forward through the debuncher for  $\sim 4000$  times. For an atom radius of 100 pm, the collision cross-section is  $3 \cdot 10^8$  b. Thus, the trapped Li ion has an average probability to be subjugated to 30 collisions with the residual gas during the 100 ms of trapping time.

During the test it was noticed that the beam current at the debuncher exit in the pass-through mode was not stable. Namely, the extracted beam current would gradually decrease from 5 nA to  $\sim 3$  nA, and then suddenly recover to the original value of 5 nA. At this beam current, the cycle period of this event was  $\sim 30$  s. By lowering the injected beam current, the cycle length was prolonged. This behavior was attributed to successive beam charging and discharging events in the debuncher. The problem was not localized, nor resolved during the test session.

*DEBUNCHING TEST*

The debunching test was also conducted with the  ${}^7\text{Li}^{+1}$  ions with injection energy of 70 eV. In order to obtain a Gaussian-like energy distribution of the injected beam a  $\sinh(t^2)$  perturbation potential delivered by an arbitrary function generator was coupled to the HV platform via a capacitor. The voltage had an amplitude of 5 V and period of 1.2  $\mu\text{s}$  (to be compared to the ion injection time of 20  $\mu\text{s}$ ). Due to the already present strong voltage oscillations and the unknown impedance of the platform, the applied potential did not have the desired shape. Nevertheless, the distribution of the resulting potential signal had a satisfying Gaussian-like projection (see Figure 5).

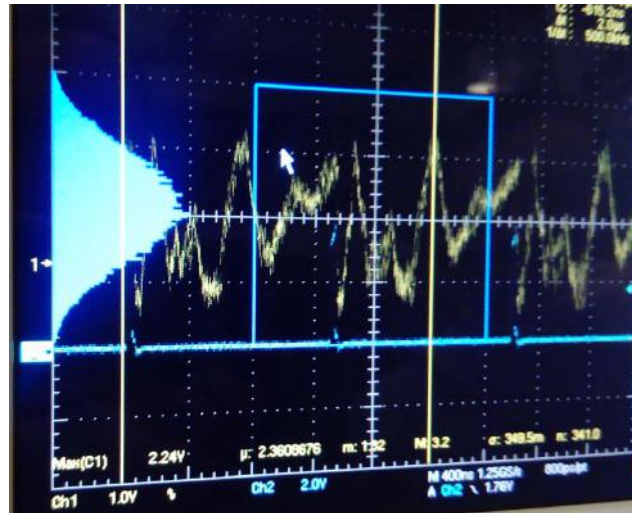


**Figure 5:** HV platform oscillations induced by the arbitrary waveform generator superimposed with the the inherent ripple from the main high voltage power supply. On the x-axis one major unit corresponds to 400 ns and on the y-axes 1 V.

The DC segment groups were ramped successively with intervals of 30 ms. The time distribution of the extracted ions is shown in Figure 6. From the top histogram of Figure 6 it can be concluded that only the second and third DC segment groups eject ions, while the other subsequent groups have a much weaker effect. In order to verify this assumption, the second ramp was delayed for 30 ms matching the ramping of the third group, and the result is shown in the middle histogram. Thereafter, both the 2<sup>nd</sup> and 3<sup>rd</sup> groups were delayed for an additional 30 ms in order to match the ramping of the 4<sup>th</sup> group (bottom histogram). The ion distribution moved 30 ms in first case and 60 ms in the second case. This confirmed that only the first two ramps eject practically all the ions in the debuncher (with exception of the first group of segments, for some reason). Such behavior is confirmed by SIMION simulations, although the first group had a certain influence on the simulations. In fact, it seems that all the Li ions spend enough time in the ramping region while the potential is raised to obtain a substantial amount of the energy sufficient to leave the debuncher. As the December 2017 test did not give satisfactory results, a different extraction approach was applied in the January 2018 test.

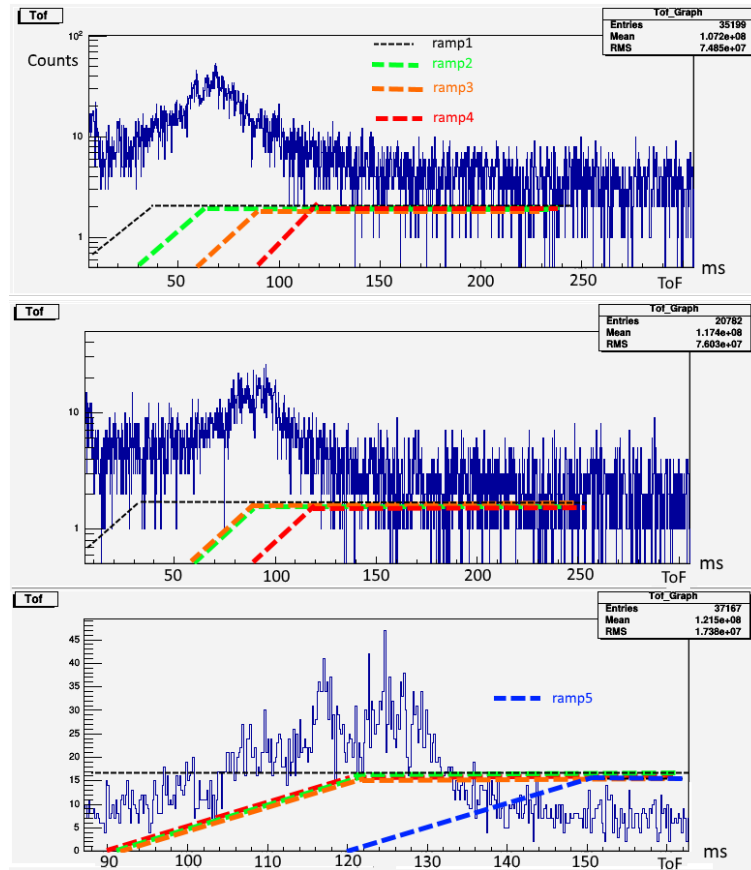


**Figure 6:** Li ions ejected by subsequent use of linear potential ramps analogue to the ones used in the EMILIE debunching test with a period time of 12.5 ms (see Figure 2).

## DEBUNCHING TEST WITH INVERSE DISTRIBUTION FUNCTION METHOD (JANUARY 2018 TEST)

### THE METHOD

In the frame of EMILIE, the ramps were applied separately to the DC segment groups, one after another (as shown in the Figure 2), resulting in the slow pulses of extracted ions. The same method was applied in the December 2017 test with little success.

Therefore, the strategy applied in January 2018 test was different. The same time-varying potential function was applied to all DC segments in the trap during the extraction phase. The function is based on the energy distribution of the ions inside the trap. The energy distribution, or actually the axial momentum distribution, of the trapped ions is first probed by linearly lowering the trapping potential, or by linearly increasing the DC potential of the inner electrodes in our case. Then, by applying the inversed integral distribution of the obtained energy distribution to all the groups of segments, it is possible to uniformly extract the ions from the debuncher. The algorithm of this method is presented in Figure 7. The test was started with the shorter trapping time of 10 ms, which was later increased to 100 ms and then up to 800 ms.

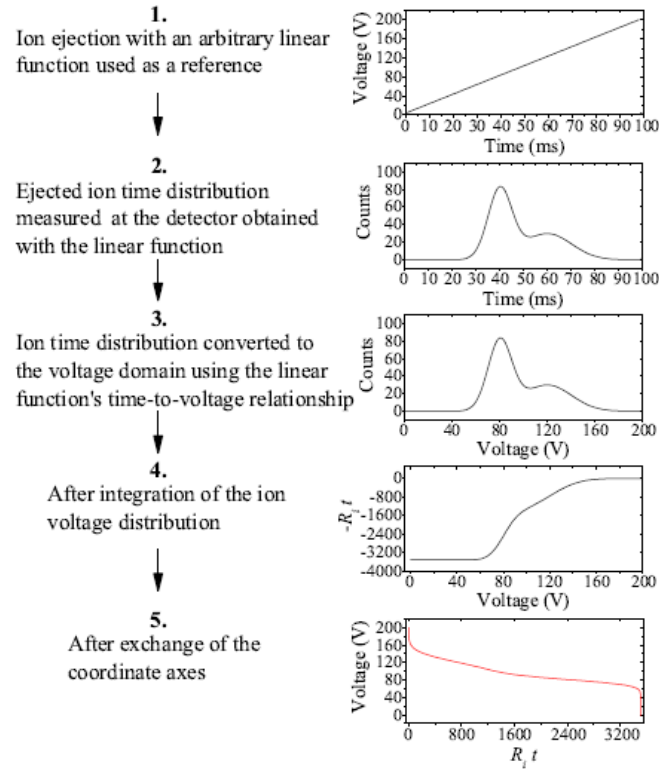


**Figure 7:** Method adapted from Lapierre [5].  $R_i$  is a constant rate of ion extraction (see [5] for details) and the  $R_i t$  corresponds to the lowering rate of the exit DC gate. Instead of lowering the potential of the exit gate, we increased the potential of the inner DC electrodes inside the trap to produce the debunched beam.

*THE EFFICIENCY TEST*

Also for the January 2018 test we conducted a trapping efficiency verification, using  ${}^7\text{Li}^{1+}$  ions with a lower injection energy into the trap ( $E=30$  eV) and a lower exit gate potential of 220 V.

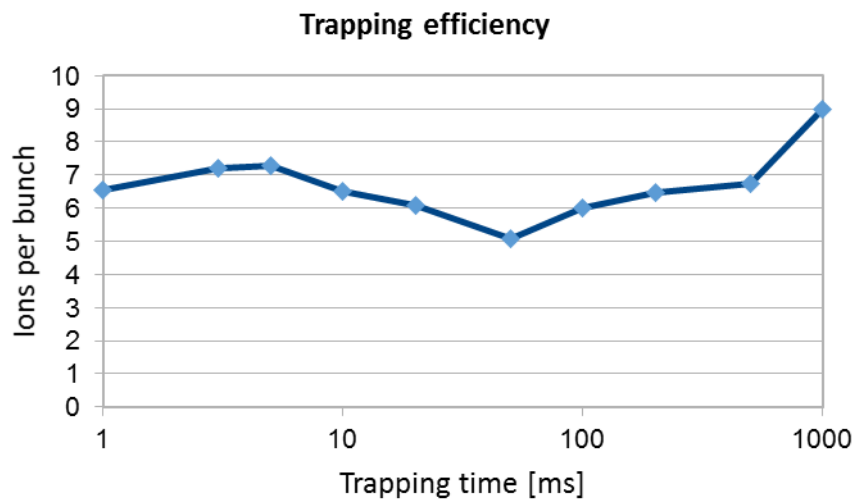


**Figure 8:** Trapping efficiency test for  ${}^7\text{Li}^{1+}$  ions with a lower ion energy (30 eV) showed that there is no significant losses at longer trapping duration, contrary to what was seen for ion energies of 70 eV (see Figure 3).

As can be seen in Figure 8, no significant losses were noticed for trapping times up to 1 s. The variation of the extracted ion intensity can be attributed to the already noticed fluctuations of the Li beam coming from the ion source, or potentially due to charging/discharging of certain parts in the debuncher being hit by the beam. The statistical uncertainty (lower than 3.5%) is too low to explain the variations. Furthermore, the energy of the ion cloud reduced with trapping time, as can be seen from the increased time-of-flight for the extraction as function of the trapping time (see Figure 9). The average velocity changes by a factor of 2 between trapping times of around 10 ms (ToF  $\sim 170 \mu\text{s}$ ) and a trapping time of 1 s (ToF  $\sim 340 \mu\text{s}$ ). An increase of the time of flight spread was additionally noticed, as shown in Figure 10. The reason for this apparent cooling effect would have to be investigated further for a better understanding of the processes involved in the debuncher. For the time being, this “cooling” effect was found to be at least harmless for trapping ions over long times, and was therefore not further investigated in the frame of this work.

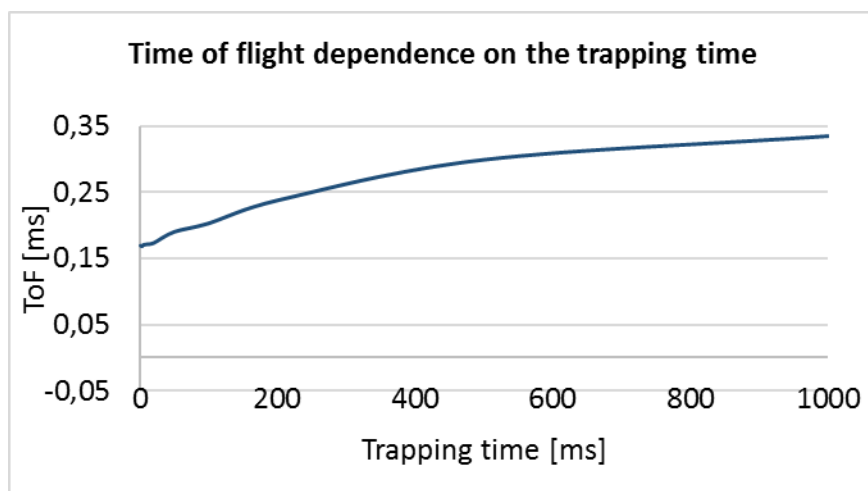


**Figure 9:** Time-of-flight as a function of the trapping time. The average ion velocity changes by a factor 2 between short trapping times (around 10 ms) and a 1 s trapping time.

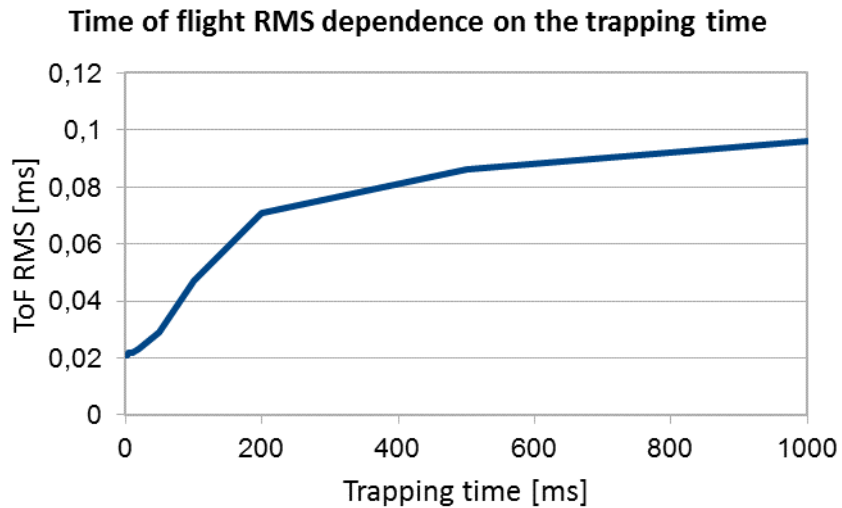


**Figure 10:** Root mean square (RMS) of the time-of-flight as a function of the trapping time.

### *THE 10 MS DEBUNCHING SIGNALS*

By ramping all segments linearly in time, from 0 V to 120 V during the trapping time of 10 ms, the axial momentum distribution shown in Figure 11 (a) was obtained. The inversed integral distribution (b) was calculated numerically, for which purpose a C++, ROOT based code was developed [6]. The inverse function was then applied to all segments during the ejection phase, yielding a nearly uniform distribution of the extracted ion beam intensity (c). Most part of the non-uniformity in the extracted beam intensity comes from the instability of the energy distribution, which most probably comes from the unstable platform potential. The potential delivered by an arbitrary function generator coupled to the HV platform was removed in the 10 ms debunching test (it was used previously in December 2017 test, and later in the 100 ms and 800ms debunching test in January 2018 – as explained in the next two sections).

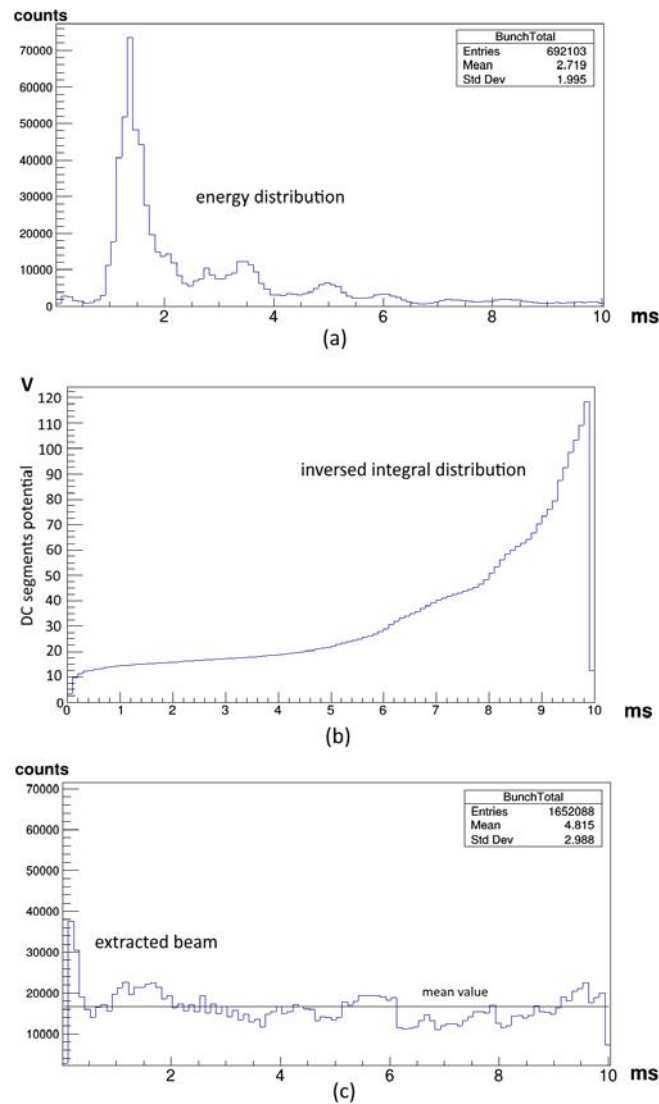


**Figure 11:** (a) The axial momentum distribution of  ${}^7\text{Li}^{1+}$  ( $E=30$  eV) measured by applying a linear ramp potential to the ejecting DC electrodes; obtained from step 2 in Figure 7. (b) The inverse integral distribution (step 5 in Figure 7) and (c) the extracted beam, which exhibits a quite uniform intensity in time.

### THE 100 MS DEBUNCHING SIGNALS

Since the 10 ms debunching test was successful, the trapping time was thereafter prolonged. Therefore, the same debunching procedure, as previously described for the 10 ms cycles, was applied for the 100 ms and also for the later described 800 ms debunching cycle – with exception that the potential generator on the HV platform ground was not used in the case of 10 ms debunching.

Due to uncontrolled variations of the energy distribution of Li ions caused by the aforementioned beam charging effect, the uniform beam extraction for trapping times of 100 ms proved to be very difficult, if not impossible. We could also observe two types of variations on the HV platform: short period variations of order of several seconds, which were visible on the oscilloscope connected to the platform via a HV probe, and longer period variations (from few seconds to several minutes) which were visible on the acquisition spectra. Thus, we introduced a variation on the HV platform ground in order to induce a controlled energy dispersion, which could decrease (in a relative sense) the influence of the parasitic potential variations. A

potential generator with periodic  $\sinh(t^2)$  function was connected to the HV platform ground, in a similar way to what was done earlier in the December 2017 tests (see Figure 5). The amplitude was increased in comparison to the December 2017 tests, so the peak to peak amplitude of the generated  $\sinh(t^2)$  function potential was  $\sim 12$  V, with an average potential of 6 V and the period of  $\sim 1.2 \mu\text{s}$ . The applied potential is shown in Figure 12 and it was synchronized with the injection period. The motivation to introduce the potential generator in December 2017 test was mainly to emulate the Gaussian energy distribution, while in January 2018 test, the motivation was to decrease the influence of the potential variations and thus, to decrease the variation of the energy distribution.

The introduction of the potential generator to the ground potential of the HV platform did not completely mask the influence of the potential variations, however, it made the test feasible.

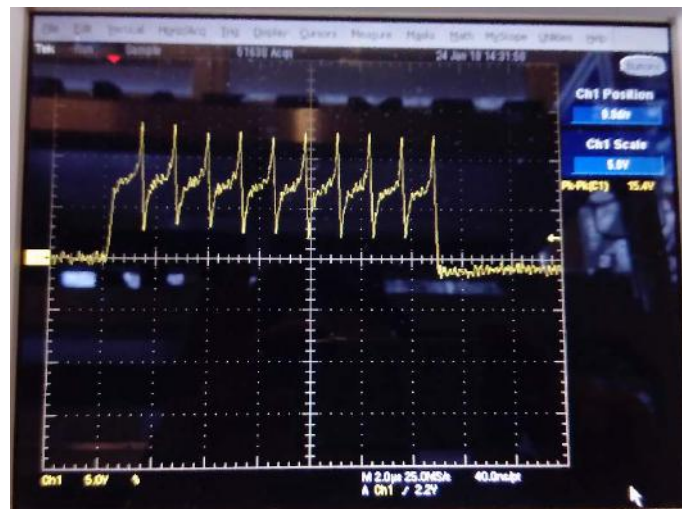


**Figure 12:** The potential introduced to the ground of the HV platform (January 2018 test), synchronized with the injection period.

This intervention allowed us to achieve a relatively uniform debunching of the beam. A certain non-uniformity was still persistent, mostly on the level of the short period variations, as it can be seen in Figure 13 and Figure 14 (left-hand part), where debunched signals are shown at two independent 100 ms extraction runs.

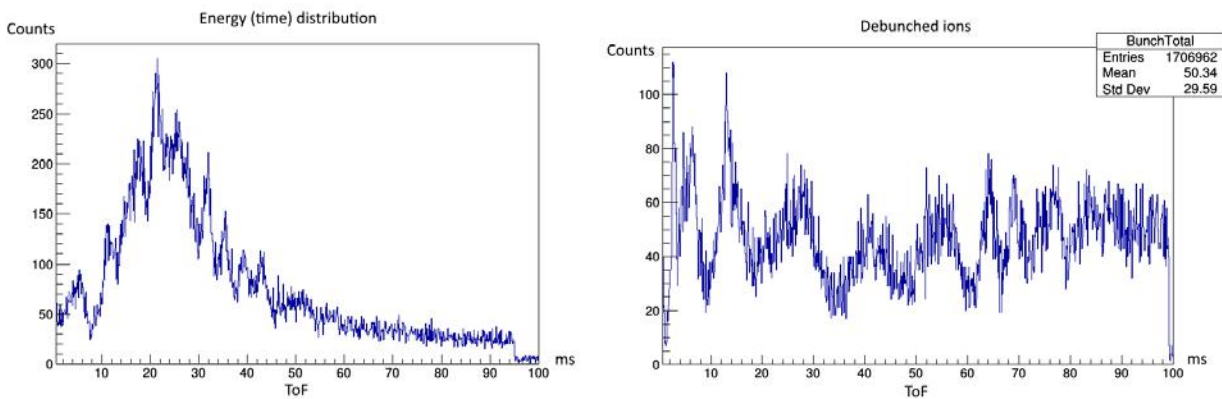


**Figure 13:** First 100 ms debunching run: The axial momentum distribution scanned by linear ramp potential during the trapping period of 100 ms (left-hand). The beam extracted by the inverse integral function (right-hand).

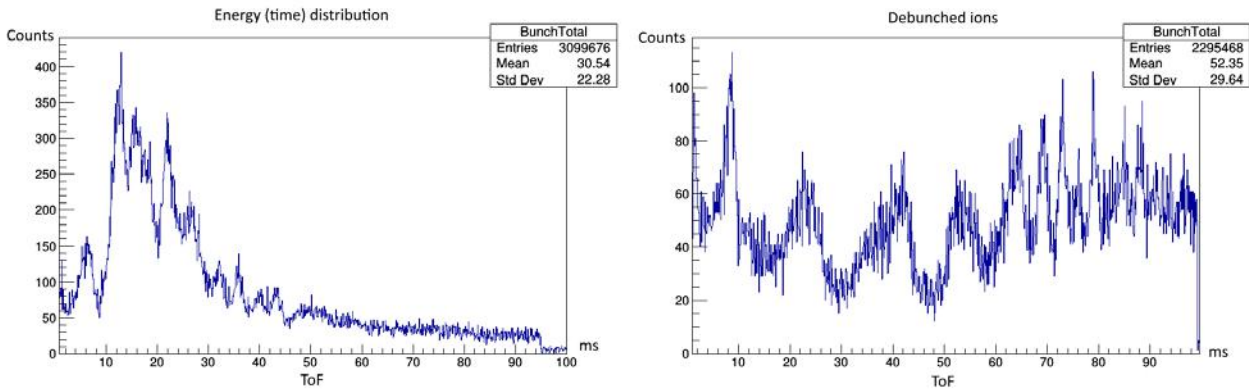


**Figure 14:** Second 100 ms debunching run: The axial momentum distribution scanned by linear ramp potential during the trapping period of 100 ms (left-hand). The beam extracted by the inverse integral function (right-hand).

By comparing Figure 13 and Figure 14, it can be noticed that the axial momentum distribution (and consequently the energy distribution) is not stable, neither by form, nor by position, which complicates the uniform extraction, although the time difference between these two runs is only 25 min. The process of the inverse function calculation and then its loading to the potential generator controlling the DC segment groups took around 20 min. Thus, at the moment of the appliance of the inverse function, it was not optimal anymore due to the change of the energy distribution occurring during the preparation of the inverse function. Nevertheless, the principles of the uniform extraction were proven.

*THE 0.8 S DEBUNCHING TEST*

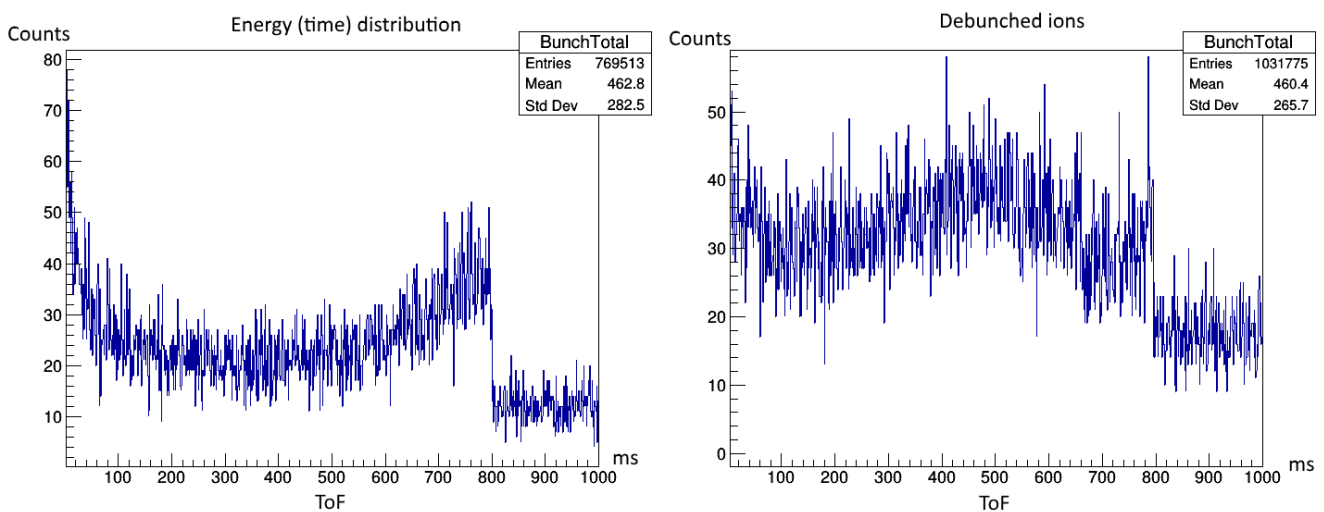


**Figure 15:** 800 ms debunching: The axial momentum distribution scanned by linear ramp potential during the trapping period of 800 ms (left-hand). The beam extracted by the inverse function (right-hand).

In the case of 800 ms cycles, it can be noticed that the ion axial momentum distribution function shown in Figure 15 (left-hand) is flat, as a consequence of a significant cooling effect during the 800 ms trapping period. However, the cooling of the Li ions due to the interactions with the atoms of the residual gas introduce a nonlinearity in the application of the inverse distribution method. This effect can partially explain the non-uniformity of the intensity of the extracted beam and it is believed that it is necessary to improve the vacuum conditions and thereby suppress the cooling effect, in order to obtain a better uniformity.

In the case of the 800 ms debunching period, the background, mostly the noise, was not negligible as in the cases for shorter trapping times (100 ms and less). It was therefore necessary to subtract the background in order to obtain the correct inverse distribution. The background is estimated during the period between two debunching cycles (between 800 and 1000 ms). The background was subtracted under the assumption that it is uniform, which is not necessarily correct and such removal of the background could have introduced an additional non-linearity in the extracted beam intensity.

## CONCLUSIONS

We successfully demonstrated the principles of uniform ion debunching in the EBIS debuncher for trapping times up to  $\sim 1$  s. The injection efficiency was estimated to be 18%, and a new dedicated ion optics should be introduced in order to increase the ion injection efficiency. No detectable losses were recorded for trapped ions with injection energies of  $\sim 30$  eV, even for longer trapping times of  $\sim 1$  s. The debunching process was delicate because of potential instabilities in the trap, probably introduced through noise on the HV platform potential.

The next steps would be to stabilize the platform potential and thereby the energy distribution of the ions introduced to the debuncher, in order to improve the uniformity of the debunching signal. The possibility to use two or three DC segment groups, for simultaneous injection and capture of a new bunch, while slowly extracting the previous one, should be considered. In this condition the debunching process would essentially be uninterrupted, i. e. completely continuous.

In summary, the tests have permitted an important proof-of-principle of the debuncher concept: the debunching process works and is efficient. In order to transform the prototype into an operational machine that could be used in combination with an EBIS, two elements are presently missing:

- An optimized ion optics, as simulated during the course of the EMILIE project [1], which should in principle permit a high injection efficiency (80% or more) in the debuncher.
- The use of dedicated NEG pumps for example, which should allow to reach the ultra high vacuum level ( $<10^{-11}$  mbar) required to avoid losses due to charge exchange.

It should be noted that even these elements are presently missing, the ion optics simulations, on one side, and the existing UHV technologies used for example in EBIS devices, on the other, give some confidence that these two aspects will not jeopardize the feasibility of the debuncher concept. As such, the proof of principle reported here clearly offers interesting perspectives for such a device to be used in combination

with existing or future EBIS sources at ISOL facilities. Such setup would be for instance of high interest to produce continuous charge bred beams for HIE ISOLDE, or for a future EBIS source at GANIL used as an injector to the CIME cyclotron. For these facilities, the debuncher would be an efficient method to drastically reduce the detection and data handling problems caused by the pulsed beam structure of the EBIS. At longer term, the benefit of such a device would be even more obvious for the intense beams to be produced at EURISOL.